JOURNAL OF GEOPHYSICAL RESEARCH, VOL. 92, NO. B10, PAGES 10,170–10,178, SEPTEMBER 10, 1987

# Local Crustal Extension at Mount St. Helens, Washington

CRAIG S. WEAVER, WENDY C. GRANT, AND JULIE E. SHEMETA

*U.S. Geological Survey, Geophysics Program AK-50, University of Washington, Seattle*

Seismicity and the orientation of fault planes from focal mechanisms indicate that Mount St. Helens is located at a dextral offset along the St. Helens seismic zone (SHZ): earthquake swarms occurring in this offset are related to volcanic eruptions. Because motion on the SHZ is in a right-lateral strike-slip sense, this dextral offset creates extension within a volume of the crust between the offset fault segments. This offset geometry is similar to that of geothermal areas along the San Andreas fault system. We apply a model derived from these geothermal areas to Mount St. Helens and find that the major differences between Mount St. Helens and the geothermal areas can be related to the ratio of the width of the offset between fault segments ($l$), to the seismogenic depth ($h$). At Mount St. Helens this ratio is $<1$, whereas in the geothermal areas the ratio is $\approx 1$. We propose that when $l/h < 1$ as at Mount St. Helens, the regional minimum principal stress does not completely dominate the small volume under extension, and as a consequence, the opening geometry is poory established compared to the oblique crustal spreading that characterizes the geothermal areas where $l/h \approx 1$. Late Quaternary volcanic vents near Mount St. Helens strike northeast, similar to the strike of a set of pre-Quaternary faults and intrusive rocks that are mapped north of the volcano; in addition, the deepest earthquakes occurring within the extensional volume are aligned along a northeast striking fault. Since these northeast striking features are aligned approximately prependicular to the regional minimum principal stress, we infer that the spatial position of Mount St. Helens is controlled by the junction of the right-stepping offset of the SHZ with the older set of fractures and that these fractures are favorably aligned with respect to the contemporary regional tectonic stress directions for the transport of magma through the brittle crust. The sense of fault motions predicted by our model for local crustal extension is consistent with an apparent component of right-lateral shear measured from geodetic lines around Mount St. Helens during June and July 1980.

## INTRODUCTION

Mount St. Helens is a Quaternary stratovolcano located in southwestern Washington along the St. Helens seismic zone (SHZ), a 100-km-long zone of moderate magnitude (up to 5.5) earthquakes that have predominately strike-slip focal mechanisms on northerly striking fault planes. The occurrence of an active volcano along the strike of an active seismic zone located within a dense seismic network provides an unusual opportunity to examine the relation between regional seismotectonics and active volcanism with a precision not often available. To date, however, earthquake studies in southwestern Washington have concentrated on defining the SHZ [*Weaver and Smith*, 1983; *Grant et al.*, 1984; *Grant and Weaver*, 1986] and on the relation between volcanic earthquakes and eruptive processes at Mount St. Helens [*Endo et al.*, 1981; *Malone et al.*, 1981, 1983; *Weaver et al.*, 1983; *McNutt and Beavan*, 1984; *Scandone and Malone*, 1985; *Shemeta and Weaver*, 1986; *Fremont and Malone*, this issue].

This paper addresses the relation between the regional seismotectonics of southwestern Washington and Quaternary volcanism at Mount St. Helens. By examining earthquake locations and focal mechanisms, we show that a change of strike occurs in the SHZ at Mount St. Helens which results in a small dextral offset of the SHZ at the volcano; eruption-related earthquake swarms occur in this offset. This relation between the seismicity on the SHZ and that directly beneath Mount St. Helens is similar to observations of the seismicity pattern in geothermal areas along the San Andreas fault system. There, earthquake swarms and volcanic and geothermal features occur within local volumes of crustal spreading that are located in dextral offsets along right-lateral strike-slip fault zones [*Hill*, 1977; *Weaver and Hill*, 1978/79]. We extend a model of local crustal spreading developed by *Weaver and Hill* [1978/79] from the observations in these geothermal areas to include the geometry of crustal extension defined by seismicity at Mount St. Helens. We suggest that the position of Mount St. Helens is the result of this crustal extensional volume intersecting a set of northeast striking fractures [*Evarts et al.*, this issue] that predate the Quaternary volcanism. Finally, we compare our local crustal extensional model and geodetic data taken during the summer of 1980 and conclude that the sense of fault motion predicted by our model can account for an apparent component of right-lateral shear that was observed across Mount St. Helens in June and July 1980.



Paper number 6B6039.
0148-0227/87/006B-6039$05.00

## SEISMOLOGICAL AND GEOLOGICAL OBSERVATIONS

### *Seismicity*

For this study we initially selected all earthquakes in the Mount St. Helens area (Figure 1) from the University of Washington catalogs that were greater than coda magnitude ($m_{coda}$) 1 and occurred between 1980 and 1985. This data set includes a very large number of earthquakes located directly beneath Mount St. Helens (rectangle in Figure 1) that were mostly shallow ($<3$ km) volcanic earthquakes associated with individual eruptive episodes including the earthquakes before the May 18, 1980, eruption. Because these shallow events are related to local eruptive processes near the current lava dome within the crater of Mount St. Helens, we have eliminated them from this data set. The remaining earthquakes were relocated following the procedures discussed by *Shemeta and Weaver* [1986]. The seismic station distribution has been relatively constant since the summer of 1980, and the station geometry has provided good resolution of hypocentral parameters; all computed hypocentral errors are less than $\pm 1.0$ km. Magnitudes were calculated from coda durations using the

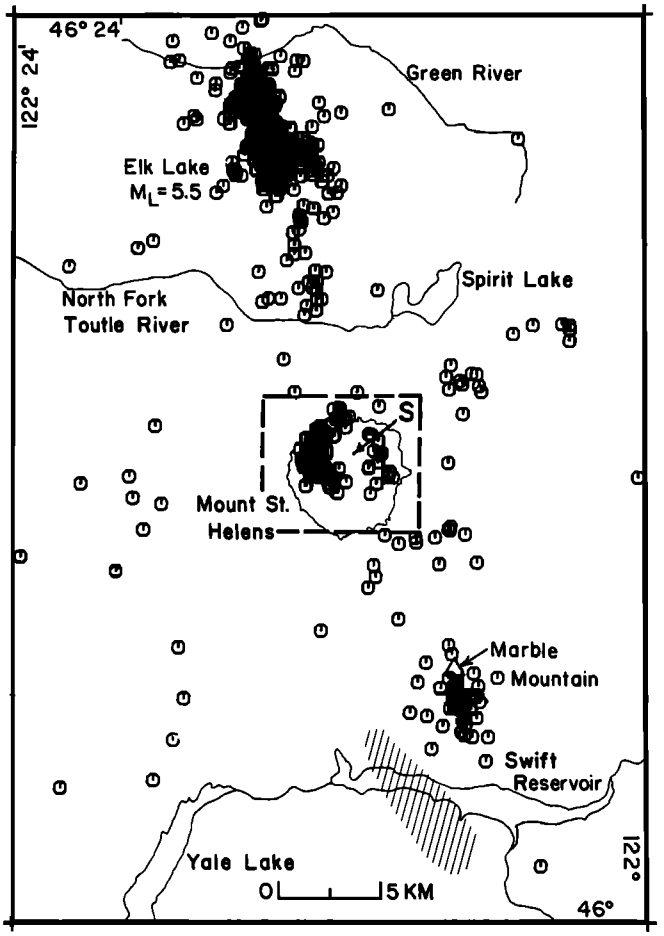


Fig. 1. Earthquakes in the vicinity of Mount St. Helens that have magnitudes greater than 1 for the period 1980–1985. Earthquakes within the dashed rectangle have been selected according to the discussion in the text. The "S" shows the general location of the injection phase of the May 18 posteruption swarm. The hatched area indicates the location of an earthquake sequence in 1960–1962 that is discussed in the text.

relation derived by *Crosson* [1972]; magnitudes of the larger events (magnitude >3.5) were calculated from the Wood-Anderson seismographs in Seattle (epicentral distance of 145 km).

*Earthquakes off the flanks of Mount St. Helens.* North of the North Fork of the Toutle River the seismicity is dominated by activity in the vicinity of the Elk Lake earthquake sequence on the SHZ (Figure 1); very few of these earthquakes are located away from the SHZ. As discussed by *Grant et al.* [1984], the Elk Lake mainshock of February 14, 1981, had $M_L = 5.5$ and had aftershocks as large as $m_{coda} = 4.5$. Nearly all of the events to the east of the main shock are part of a precursory swarm of earthquakes (including three with $m_{coda} \geq 4$) that occurred from May to July 1980 [*Grant et al.*, 1984]. Based on the distribution of the earthquakes into a precursory swarm zone and an aftershock zone at Elk Lake, *Grant et al.* [1984] concluded that the SHZ north of Mount St. Helens consisted of a series of short, parallel fault zones, rather than a single fault trace. Fewer earthquakes are located between the southern end of the Elk Lake aftershock zone and Mount St. Helens; however, the epicenters of these earthquakes follow the average strike of the aftershock zone. The depth of the seismogenic zone of the SHZ is about 16 km except directly beneath the north slope of Mount St. Helens. Here earthquakes with focal depths as deep as 20 km occurred on May 18–19, 1980 [*Shemeta and Weaver* 1986; *Scandone and Malone*, 1985].

Fewer earthquakes occurred south of Mount St. Helens than to the north, and all earthquakes to the south are located above 12 km in depth. Unlike the Elk Lake area where the rate of background seismicity is relatively high, few earthquakes occurred south of Mount St. Helens that were not associated with a July–August 1980 swarm of small magnitude (largest $m_{coda} = 3.6$) earthquakes near Marble Mountain [*Grant and Weaver*, 1986]. South of Marble Mountain, the strike of earthquake hypocenters indicates that the SHZ is offset to the west by several kilometers and strikes to the southeast across Swift Reservoir (Figure 1). The earthquakes along this southern segment were part of a sequence that occurred during 1960–1962; this sequence included five events greater than magnitude 4, with the largest earthquake of $M_L = 5.1$ [*Grant and Weaver* 1986]. Due to the paucity of seismic stations only the larger magnitude earthquakes in this sequence could be located.

Since 1980 the few earthquakes located off the SHZ (Figure 1) have all been of small magnitude (only one event had $m_{coda} > 2.5$). To the west and southwest of Mount St. Helens, the activity is diffuse, although the events could represent a still poorly defined zone that strikes to the north parallel to the SHZ. East of Mount St. Helens, there are three small groups of earthquakes; two groups are approximately 5 and 10 km northeast of the volcano, and the third group is approximately 5 km southeast of the crater. The largest magnitude (3.7) event since 1980 outside of the Elk Lake area occurred in this southeastern group.

*Earthquake distribution beneath Mount St. Helens.* After removing the shallow ($\leq$ 3 km) volcanic earthquakes from the data set, nearly all of the remaining events beneath Mount St. Helens are part of posteruption swarms that followed the explosive eruptions of 1980: the earthquakes following the May 18 eruption clearly dominate this data set (Figure 2). These posteruption earthquakes can be subdivided into two distinct volumes on the basis of hypocentral depth. One volume is between 3 and about 7.5 km, whereas the second volume is between 7.5 and about 20 km in depth. Between 3 and 7.5 km in depth, the earthquakes beneath the crater of Mount St. Helens cluster in a tight distribution about 1 km in radius [*Shemeta and Weaver*, 1986; *Scandone and Malone*, 1985]. *Shemeta and Weaver* [1986] interpreted these earthquakes as surrounding a narrow conduit connecting the surface with the deeper magma system below 7.5 km. Because these earthquakes are the result of the injection of magma from depth into the narrow conduit during the eruption we will refer to these events as the injection swarm. For clarity, we have shown the location of the injection swarm schematically (S in Figure 1) so that we can emphasize the locations of the earthquakes below the injection swarm volume.

The injection swarm began with the onset of the May 18 eruption and lasted about 9 hours. The swarm was particularly intense during the late afternoon on May 18 as over half of the total seismic moment released in the 48 hours following the onset of the May 18 eruption occurred during the injection swarm within a period of 45 min [*Shemeta and Weaver*, 1986]. The seismicity associated with the injection swarm decayed rapidly after the eruption stopped [*Shemeta and Weaver*, 1986]. The largest magnitude earthquake recorded in this swarm had $M_L = 4.5$. Although a very few earthquakes oc-

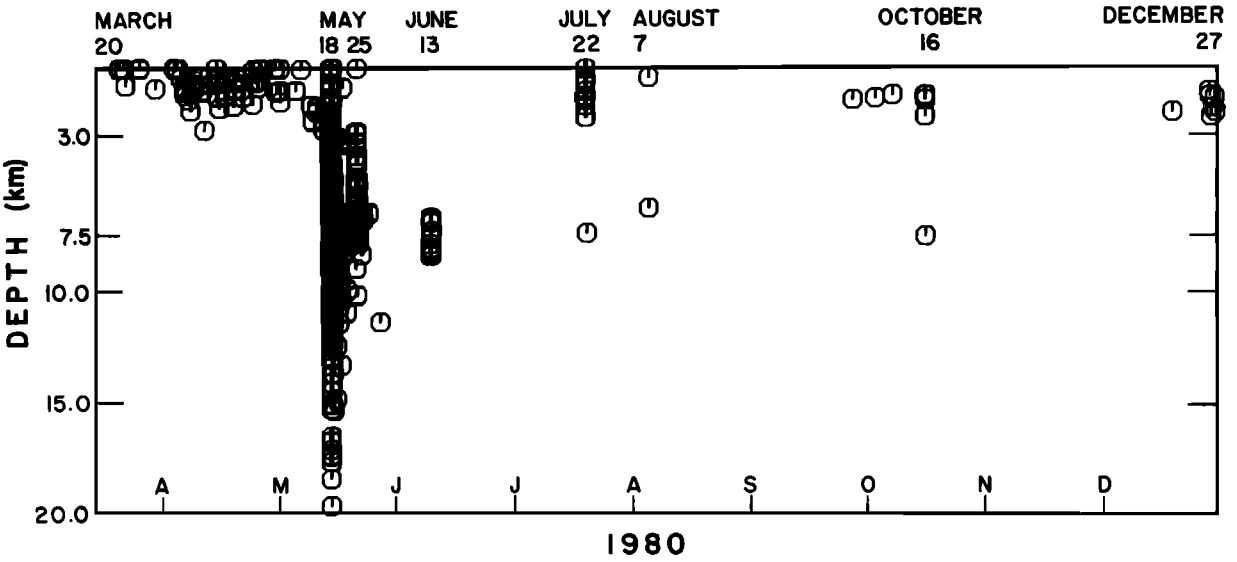


Fig. 2. Time-depth plot of earthquakes within the dashed rectangle in Figure 1. All earthquakes less than 3.0 km are volcanic events related to the individual eruptive episodes and are not plotted in Figure 1.

curred between 3 and 7.5 km depth after the May 25 eruption, all of the significant activity in this depth range occurred as part of this injection swarm that followed the May 18 eruption (Figure 2).

After deleting both the volcanic earthquakes (<3 km) and the injection swarm earthquakes (3–7.5 km), the earthquakes plotted beneath Mount St. Helens in Figure 1 are in the deeper volume; most of these events followed the May 18 eruption, although a few events followed the eruptions on May 25 and June 13 (Figure 2). These deeper events define an earthquake-free volume (Figure 1) beneath the positon of the vent. This earthquake-free volume has been suggested as the location of a deep magma reservoir [*Scandone and Malone*, 1985; *Shemeta and Weaver*, 1986]. Because most of these deeper earthquakes occurred after the eruptions ceased, they have been interpreted as representing the adjustment of country rock surrounding the magma reservoir to magma withdrawal [*Malone and Scandone*, 1985; *Shemeta and Weaver*, 1986]. *Shemeta and Weaver* [1986] interpret the earthquakes surrounding this earthquake-free volume between 7.5 and 20 km as occurring on a northeast striking fault that bounds the earthquake-free zone on the northwest and a nearly north-south striking fault from 7.5 to 12 km depth that bounds the earthquake-free volume to the east (Figure 1). We

TABLE 1. Focal Mechanism *P* and *T* Axes

| ID | Date | Time | Latitude | Longitude | Depth, km | *M* | Reference | *P* Axis | | *T* Axis | |
|---|---|---|---|---|---|---|---|---|---|---|---|
| | | | | | | | | Strike | Dip* | Strike | Dip* |
| S1 | May 18, 1980 | 2354 | 46°12.70'N | 122°12.61'W | 12.85 | 3.2 | 3 | N070°E | 37° | N110°W | 55° |
| S2 | May 19, 1980 | 0057 | 46°12.97'N | 122°12.24'W | 13.76 | 3.9 | 3 | N163°W | 36° | N059°W | 19° |
| S3 | May 19, 1980 | 0131 | 46°12.54'N | 122°12.37'W | 11.22 | 3.7 | 3 | N001°E | 06° | N096°W | 37° |
| S4 | May 19, 1980 | 0136 | 46°12.25'N | 122°10.16'W | 8.38 | 2.6 | 3 | N010°W | 24° | N133°E | 60° |
| S5 | May 19, 1980 | 0351 | 46°11.90'N | 122°10.58'W | 9.07 | 2.3 | 3 | N124°W | 4° | N032°W | 25° |
| S6 | May 19, 1980 | 1421 | 46°13.04'N | 122°12.40'W | 13.75 | 3.9 | 3 | N153°E | 14° | N073°W | 70° |
| S7 | May 19, 1980 | 1820 | 46°13.04'N | 122°12.51'W | 13.85 | 2.1 | 3 | N155°E | 12° | N083°W | 68° |
| S8 | May 20, 1980 | 1234 | 46°12.53'N | 122°12.35'W | 12.36 | 3.4 | 3 | N089°E | 62° | N073°W | 26° |
| S9 | May 21, 1980 | 0821 | 46°11.81'N | 122°12.31'W | 9.57 | 2.7 | 3 | N002°E | 3° | N092°E | 3° |
| 10 | Feb. 14, 1981 | 0609 | 46°20.96'N | 122°14.16'W | 7.28 | 5.5 | 1 | N040°E | 10° | N050°W | 2° |
| 11 | May 24, 1980 | 2301 | 46°20.02'N | 122°12.99'W | 1.63 | 4.1 | 1 | N130°W | 4° | N137°E | 10° |
| 12 | July 25, 1980 | 0542 | 46°18.94'N | 122°12.94'W | 3.45 | 2.5 | 3 | N160°W | 18° | N066°W | 4° |
| 13 | Sept. 5, 1980 | 0345 | 46°18.28'N | 122°13.12'W | 3.44 | 2.7 | 3 | N015°E | 7° | N106°E | 7° |
| 14 | June 3, 1980 | 0542 | 46°17.19'N | 122°12.50'W | 1.19 | 2.7 | 3 | N147°W | 7° | N123°E | 7° |
| 15 | Dec. 18, 1981 | 0919 | 46°16.28'N | 122°12.24'W | 2.41 | 2.7 | 3 | N034°E | 7° | N057°W | 7° |
| 16 | Nov. 25, 1982 | 0645 | 46°14.69'N | 122°07.34'W | 8.38 | 2.2 | 3 | N150°W | 12° | N059°W | 3° |
| 17 | May 4, 1981 | 1747 | 46°15.32'N | 122°02.85'W | 11.59 | 2.1 | 3 | N136°W | 44° | N034°W | 12° |
| 18 | July 20, 1980 | 1422 | 46°10.33'N | 122°07.38'W | 8.69 | 3.7 | 3 | N159°W | 13° | N061°W | 28° |
| 19 | July 20, 1980 | 1741 | 46°06.06'N | 122°07.17'W | 4.48 | 3.1 | 3 | N025°E | 8° | N068°W | 21° |
| 20 | July 20, 1980 | 0203 | 46°05.90'N | 122°07.29'W | 4.99 | 3.5 | 2 | N026°E | 8° | N066°W | 22° |
| 21 | July 7, 1980 | 0145 | 46°05.40'N | 122°06.82'W | 4.15 | 3.2 | 3 | N014°W | 1° | N114°E | 14° |
| 22 | July 7, 1980 | 0134 | 46°05.23'N | 122°06.81'W | 4.72 | 3.1 | 3 | N151°W | 28° | N116°E | 13° |
| 23 | Sept. 17, 1961 | 1555 | 46°01.50'N | 122°06.06'W | 21.84 | 5.1 | 2 | N018°E | 20° | N112°E | 7° |

ID refers to Figure 3.

*Dip measured as degrees up from horizontal.

†References: 1, *Grant et al.* [1984]; 2, *Grant and Weaver* [1986]; and 3, this paper.

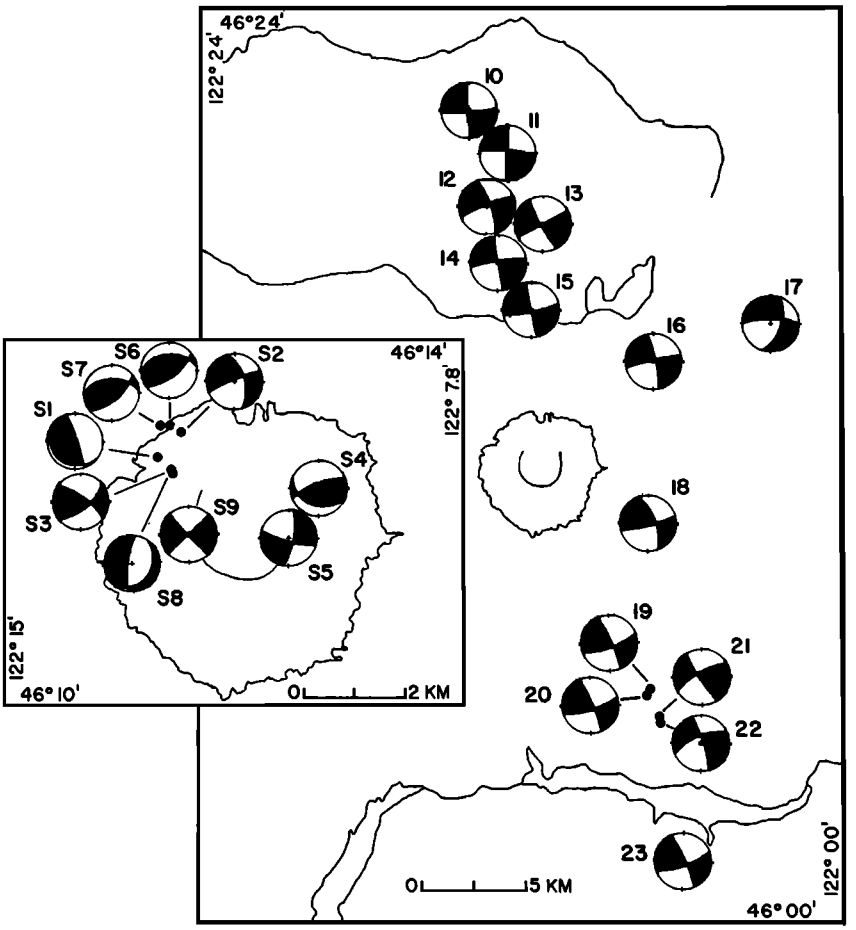


Fig. 3. Representative earthquake focal mechanisms in the vicinity of Mount St. Helens. Focal mechanisms are upper hemisphere, with darkened quadrants indicating compression and white quadrants indicating dilation. Events are keyed by number to Table 1 which gives data sources for events from other studies and $P$ and $T$ axis orientations for the mechanisms determined in this study.

will refer to the events in the second, deeper volume as the adjustment swarm.

The adjustment swarm followed the largest earthquakes in the injection swarm [*Shemeta and Weaver*, 1986] with small-magnitude (<2) deep earthquakes continuing to occur between the May 18 and May 25 eruptions. All of the deep events following the June 13 eruption were of small magnitude (<2) and occurred within the same volume as the May 18 adjustment swarm events. The largest magnitude earthquake in the adjustment swarm following the May 18 eruption had $M_L = 4.0$.

*Focal Mechanisms*

The focal mechanisms that we have compiled for this study are from both previously published studies and newly calculated. Because the focal mechanisms are all nearly identical for the Elk Lake activity [see *Grant et al.*, 1984], we have chosen only two representative mechanisms; the mechanisms for the 1981 main shock and one of the 1980 precursory swarm events (Table 1). Between Mount St. Helens and the Elk Lake aftershock zone six new mechanisms were calculated (events 12–17 in Table 1). South of Mount St. Helens, we calculated three new mechanisms for earthquakes near Marble Mountain (Table 1); in addition, we have shown one event near Marble Mountain and the main shock from the sequence south of Swift Reservoir that were calculated by *Grant and Weaver* [1986]. We recalculated mechanism "*f*" of *Weaver and Smith* [1983] because the $P$ and $T$ axis were published incorrectly (Table 1, event 18). Finally, we have included selected focal mechanisms from earthquakes occurring directly beneath Mount St. Helens. We have deleted focal mechanisms for those events above 7.5 km in depth that are interpreted to be associated with the conduit. The resulting nine mechanisms (Figure 3, insert) include six events along the northeast-striking fault that bounds the inferred magma reservoir, two events to the east of the lava dome, and one event directly west of the lave dome. All of the events are identified in Figure 3 and Table 1.

Along the SHZ north of Mount St. Helens, the focal mechanisms have north-south fault planes with strikes that are in good agreement with the average strike of the earthquake epicenters. Because of this agreement, we conclude that the north-south striking plane represents the slip plane; similar conclusions were reached by *Weaver and Smith* [1983] regarding the entire SHZ and *Grant et al.* [1984] regarding the Elk Lake activity. The scattered earthquakes to the east of Mount St. Helens have focal mechanisms that are nearly identical to those at Elk Lake; therefore we conclude that these events are likely occurring on short fault segments that strike north-south.

South of Mount St. Helens, the northerly striking fault plane of most focal mechanisms has a westward rotation of

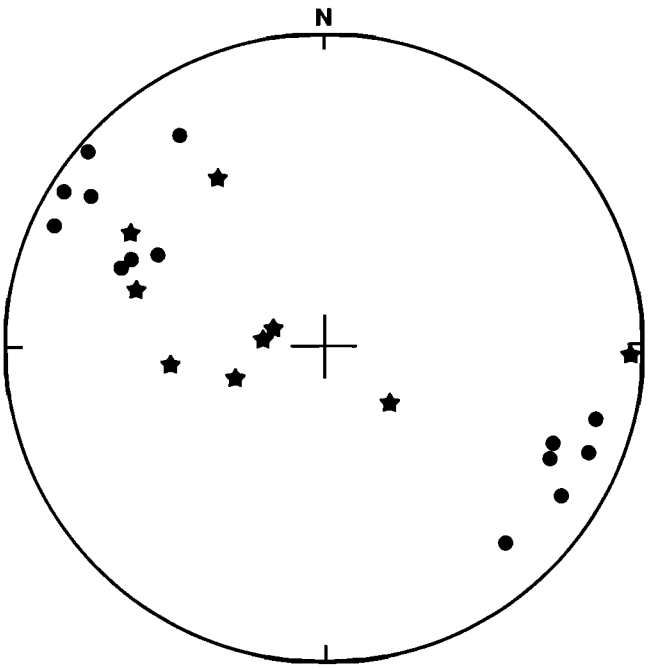


Fig. 4. $T$ axes for earthquake focal mechanisms. Stars are the $T$ axes for the earthquakes beneath Mount St. Helens (events S1–S9 in Figure 3 and Table 1), solid circles are the $T$ axes for earthquakes along the SHZ and east of Mount St. Helens (event 10–23 in Figure 3 and Table 1).

about 20° from the north-south slip planes observed north and east of the mountain. Because northerly striking fault planes are very tightly constrained by the distribution of seismic stations in western Washington, we regard this rotation as significant (see *Grant et al.* [1984] and *Grant and Weaver* [1986] for detailed focal mechanism plots). The events near Marble Mountain have well-constrained focal mechanisms and are nearly pure strike-slip on fault planes striking either north-northwest of east-northeast (Figure 3). Because the earthquakes are approximately aligned to the northwest, we choose this as the fault plane. To the south and west, the focal mechanism for the 1961 $M_L = 5.1$ event is nearly identical to those calculated at Marble Mountain. Since the located events in this sequence were aligned to the north-northwest, the northwesterly striking fault plane is the preferred slip plane for this event [*Grant and Weaver*, 1986].

From the above rotation in both the strike of the fault planes and seismicity, it is apparent that Mount St. Helens is located at or near a slight shift in the orientation of fault segments along the SHZ. North of the volcano, the preferred slip plane strikes nearly north-south, whereas to the south this slip plane is rotated to the northwest. The strikes of the nodal plane for earthquakes occurring directly beneath Mount St. Helens (Figure 3 inset) generally are similar to either the north-south (or east-west) direction or the northwest-southeast direction. Despite the rotation of the slip planes calculated from the focal mechanisms along the SHZ and a mixture of focal mechanism types directly beneath Mount St. Helens, the azimuth of the $T$ axes of all events are grouped tightly around the northwest-southeast direction (Figure 4). From a study of regional focal mechanisms data, *Weaver and Smith* [1983] inferred that this was the direction of minimum principal stress ($\sigma_3$) in southwestern Washington.

*Geological Structures*

Generally, volcanism is related to extensional processes and both theoretical and observational studies have shown that volcanic vents and cinder cones align perpendicular to the direction of $\sigma_3$. Mapped field examples of this relation include the pattern of dikes at Spanish Peaks, Colorado [*Ode*, 1957; *Pollard and Mueller*, 1976], the Quaternary rhyolite domes at the Coso Range, California [*Bacon et al.*, 1980; *Duffield et al.*, 1980], and the distribution of cinder cones around the large composite volcanoes of Alasaka [*Nakamura*, 1977]. This obsevation also holds at Mount St. Helens where the distribution of late Quaternary volcanic vents near Mount St. Helens is elongated approximately in a northeast direction (Figure 5). This distribution of vents near Mount St. Helens is similar to the vent distribution at Coso and those surrounding the Alaskan volcanoes, where the vents are aligned approximately parallel to the inferred regional principal maximum stress direction and perpendicular to the inferred regional principal minimum stress direction [see *Weaver and Smith*, 1983]. The northeast striking fault zone defined by the adjustment swarm

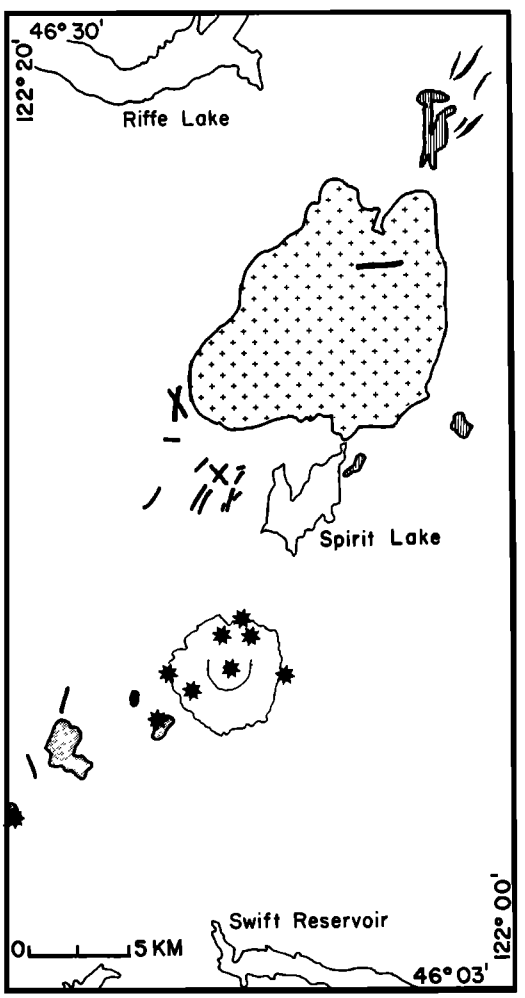


Fig. 5. Geologic evidence for northeast fractures. Stars are the position of late Quaternary vents, taken from *Luedke and Smith* [1982] and *Evarts et al.* [this issue]. The Spirit Lake pluton is indicated by the cross pattern. Irregular-shaped bodies with lined shading are small felsic intrusions; dark-shaded bodies are dacite plugs and domes. Single bold lines indicate mapped faults, lenticular bodies north of the Spirit Lake pluton represent mapped Tertiary dikes. All these features are from *Evarts et al.* [this issue].

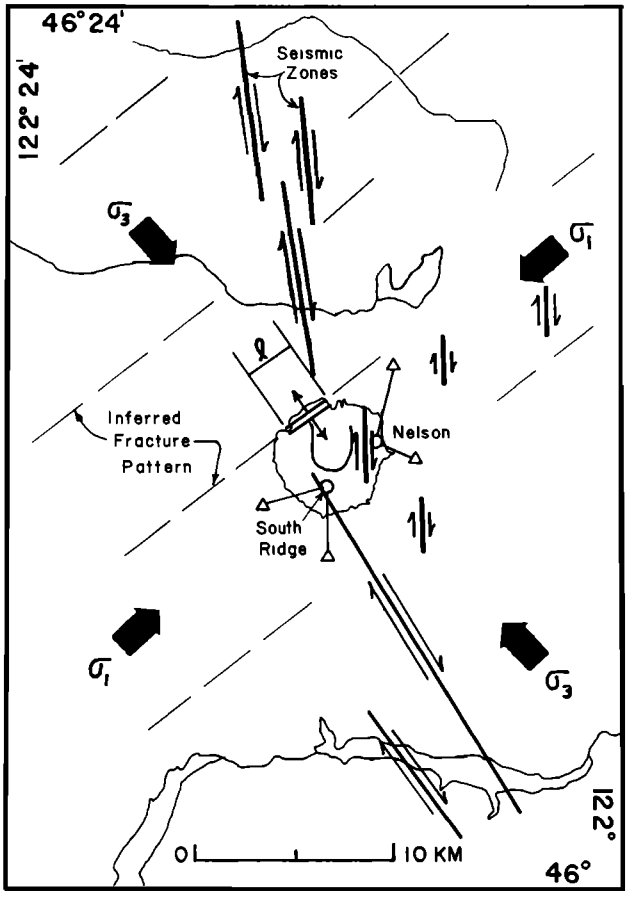


Fig. 6. Model of crustal spreading at Mount St. Helens. North striking bold lines represent segments of the SHZ, with small arrows showing the slip direction. Light, northeast striking lines are a schematic representation of the fracture pattern inferred from the orientation of the volcanic vents, air photo lineaments, and the seismic fault zone beneath Mount St. Helens. Bold arrows indicate the directions of the regional minimum ($\sigma_3$) and maximum ($\sigma_1$) principal stresses from *Weaver and Smith* [1983]. The northeast striking fault beneath Mount St. Helens is indicated with the double line. Geodetic lines discussed in text are taken from *Swanson et al.* [1981] with small triangles representing instrument sites and the open circles representing reflectors; "*l*" is the dimension of the dextral offset.

about 2 km north of the recent vent of Mount St. Helens falls on the alignment of late Quaternary vents, and a prominent topographical lineament east of the volcano parallels to the vent trend [*Evarts et al.*, this issue].

The strike of the volcanic vents at Mount St. Helens intersects a subtle geological structure that strikes more northerly (N25°E) than the vent distribution [*Evarts et al.*, this issue]. This structure was defined by *Evarts et al.* [this issue] on the basis of the set of faults north of Mount St. Helens that cut mid-Tertiary volcanic and sedimentary rocks, a series of small dikes, sills, and irregular-shaped intrusive bodies that have also cut through the mid-Tertiary rocks and prominent air photo lineaments within the Spirit Lake pluton. The Miocene-aged Spirit Lake Pluton is elongated to the north-northeast, approximately on strike with other features comprising the subtle geological structure (Figure 5). Thus *Evarts et al.* [this issue] concluded that Mount St. Helens was located at the intersection of two underlying structural trends. The vent alignment trend was interpreted by *Evarts et al.* [this issue] as related to current tectonic stresses, whereas the second more northerly trend was interpreted as a deep-seated lithospheric flaw that predates the mid-Tertiary intrusions that has been reactivated in response to contemporary tectonic stresses.

## Interpretation and Application of a Crustal Spreading Model

We interpret the seismicity data near Mount St. Helens as indicating that a small dextral offset occurs in the SHZ across the position of the volcano (Figure 6). Earthquake swarms related to volcanic eruptions of Mount St. Helens occur within this volume, and because of the fault offset this small volume is under local crustal extension. Located within this offset is the northeast striking fault that bounds the magma reservoir to the northwest and extends to a depth of 20 km. Based on the distribution of volcanic vents and the mapping of *Evarts et al.* [this issue], we infer that the northeast striking fault zone is part of a set of tectonically activated features of similar strike.

The occurrence of earthquake swarms within the dextral offset of the SHZ across Mount St. Helens is similar to areas along the greater San Andreas fault system where earthquake swarms occur within offsets between parallel strands of right-lateral strike-slip faults [*Weaver and Hill*, 1978/79]. In many cases, these offsets contain evidence that the area of the crust within the offset (approximately 5–10 km wide) between fault segments is under extension; geothermal features, normal faulting, and volcanic vents are localized within these offsets. These areas have been referred to as leaky transform faults [*Hill*, 1977] or local crustal spreading centers [*Weaver and Hill*, 1978/79].

Because strike-slip faulting is a ubiquitous feature in volcanic arcs of most subduction zones that have a continental overriding plate [*Jarrard*, 1986], it is of interest to develop a model linking arc volcanoes and strike-slip zones. The fact that earthquake swarms occur within dextral offsets at Mount St. Helens and along the San Andreas system suggests that the crustal-spreading model developed for the San Andreas may be appropriate for Mount St. Helens. This crustal-spreading model was based on six seismological and geometrical relations observed in dextral offsets where earthquake swarms were frequent. Because these areas do not have active volcanoes, it is of interest to compare the observations at Mount St. Helens with the seismological and geometrical relations derived from the San Andreas geothermal areas. In the following discussion, we will refer to the crustal spreading model as the San Andreas model.

Three relations in the San Andreas model concerned parameters of earthquake swarms. Earthquake swarms were localized to the volume of crust between the offset fault strands, the duration of earthquake swarms were limited to time scales of a few hours to a week, and the maximum magnitude of earthquakes within the swarm volume was in the range of 4.5–4.7, with the difference between the largest magnitude event and the next largest event in the swarm less than 0.5 magnitude units.

Aside from the earthquake swarms that followed each of the explosive eruptions in 1980, there have been two other earthquake swarms in the vicinity of Mount St. Helens. The largest of these swarms was at Elk Lake, and this swarm was part of a precursory seismicity sequence related to the Elk Lake main shock [*Grant et al.*, 1984]. *Grant et al.* [1984] interpreted this swarm within the context of an asperity model, relating the swarm to the distribution of fault strength around the asperity

rather than to the geometry of the fault segments. As the geothermal model is related to geometrical aspects of fault segments, we discount the Elk Lake swarm in applying the San Andreas model to the Mount St. Helens area. The second swarm sequence not directly beneath Mount St. Helens occurred in July 1980 near Marble Mountain (Figure 1). This swarm occurred in an area that may be under local crustal extension, since the SHZ is stepped westward south of Marble Mountain, and the crustal spreading model predicts that earthquake swarms should occur in this offset. Thus, disregarding the Elk Lake swarm, we conclude that earthquake swarms in the vicinity of Mount St. Helens are concentrated in dextral offsets where crustal extension is expected. From the above discussion of the May 18 swarms, both the duration of the earthquake swarms and the maximum magnitude events beneath Mount St. Helens are similar to swarm duration and maximum magnitudes observed along the San Andreas. The difference in magnitude with respect to the next largest event ($\approx$0.2 units) in the St. Helens swarms is also in accord with the San Andreas observations.

Two relations in the San Andreas model were related to the ratio of the offset dimension ($l$), between parallel strands of a fault to the depth of the seismogenic zone ($h$). Along the San Andreas system, both dimensons are typically of the order of 5–10 km, thus $l/h \approx 1$. At Mount St. Helens the offset dimension is approximately 3 km, whereas the seismogenic depth is nearly 20 km, thus $l/h < 1$. Second, *Weaver and Hill* [1978/79] noted that along the San Andreas where the ratio $l/h \approx 1$, crustal spreading occurs in areas that are oblique to the strike-slip faults. Mount St. Helens, with $l/h < 1$, lacks the oblique spreading geometry found along the San Andreas, and evidence of extension must be inferred from a small offset in the SHZ and the presence of volcanic vents.

The sixth relation along the San Andreas fault was that earthquake focal mechanisms showed little variation in the direction of the $T$ axes, with the direction remaining essentially constant along the parallel strike-slip faults and within the spreading volume. As is apparent in Figure 4, the plunges of the $T$ axes vary considerably, from nearly horizontal to nearly vertical. However, as noted above, the azimuths of the $T$ axes calculated for earthquakes occurring on May 18–19, 1980, in the offset volume are generally in agreement with the azimuth of the $T$ axes calculated for earthquakes along the strike-slip segments of the SHZ.

Based on the above comparison, it is apparent that the model of local crustal spreading developed for geothermal areas along the San Andreas is applicable to Mount St. Helens if the seismological relations in the model of *Weaver and Hill* [1978/79] are extended to include the case when $l/h < 1$. The ratio $l/h$ is apparently a sensitive indicator of the stress state and geometry in the fault offset. We propose that when $l/h < 1$, as is the case at Mount St. Helens, this indicates that a small volume is under local crustal extension and that the relation between this extensional volume and the offset strike-slip zones is poorly defined. Presumably, because the geometry between the strike-slip zones and the extensional volume is poorly defined, the $T$ axes orientations are not as invariant as when $l/h \approx 1$, and features typical of crustal spreading centers such as normal faulting may not be observed in the offset. It is likely that when $l/h < 1$ the regional minimum principal stress does not dominate the local stress conditions in the fault offset. As the ratio $l/h$ increases to values $\approx 1$, the volume under local extension can now be classified as a spreading volume, with the development of normal faulting and an oblique opening geometry. These conditions indicate that the minimum principal stress now dominates in the fault offset. As a consequence, the sixth relation of *Weaver and Hill* [1979], that the $T$ axes were nearly invariant both along the strike-slip zones and within the spreading volume, is observed for earthquake focal mechanisms. Finally, when $l/h \gg 1$ as along the oceanic ridge system, crustal spreading occurs along entire plate boundaries and the direction of crustal spreading is orthogonal to the linear spreading ridges.

In addition to the ratio $l/h$, a second difference in comparing Mount St. Helens with the geothermal areas is that the earthquake swarms at Mount St. Helens are obviously related to large volcanic eruptions, whereas this is not the case in the geothermal swarms. However, *Hill* [1977] noted that earthquake swarms within spreading volumes could be generated by several processes, but the result of the different swarm processes would not necessarily be distinguishable in earthquake locations and focal mechanism studies. This observation holds for the May 18 posteruption swarm, where at least two distinct processes (injection and adjustment) resulted in short-lived earthquake swarms that satisfy the seismological relations of the model.

## DISCUSSION

Because Mount St. Helens is a very young volcanic system less than 50,000 years old [*Mullineaux and Crandell*, 1981], it provides a particularly good example of the inception of a composite volcano within a strike-slip arc environment. The deepest earthquakes beneath the volcano indicate that magma transport probably originated along a preexisting zone of weakness that is preferentially oriented with respect to contemporary regional tectonic stresses. As is apparent from the distribution of late Quaternary vents, the inception of a volcanic center may occur at several places along a system of fractures, but longevity of the volcanic center apparently occurs only if a favorable fault geometry exists that will allow the development of crustal extension. We suggest that as a result of the opening of the brittle portion of the crust, the magma volume increases to the point that periodic eruptions from the system become possible. The repeated eruption within the extensional volume ultimately gives rise to a composite volcano, with a series of closely spaced vents (Figure 5).

Although we have developed a model for the interaction between crustal seismotectonics and the development of local crustal extension at Mount St. Helens, there are no seismological constraints on the source of the magma below the brittle portion of the crust. We do not discount the importance of the deeper magmatic sources in establishing a volcanic center, but note that both the seismic data and geological data independently indicate the importance of tectonic control and activation of structures that predate Quaternary volcanism at Mount St. Helens. *Evarts et al.* [this issue] noted that the distribution of volcanic vents at Mount St. Helens was consistent with the classification of *Bacon* [1985] for vent distributions controlled by regional tectonic stresses.

In the vicinity of Mount St. Helens the confinement of earthquake activity largely to the SHZ indicates that most of the coseismic fault slip is localized to this zone. We hypothesize that the limited number of additional late Quaternary volcanic vents near Mount St. Helens is the result of the localization of fault slip, both seismic and aseismic, to the SHZ. In regard to this latter point, it is of interest to note that the

position of the SHZ may be related to regional structure not apparent on surface geologic maps. *Stanley et al.* [this issue] and *Finn and Williams* [this issue] report that an aeromagnetic low is coincident with the strike of the epicenters of the SHZ, and *Stanley et al.* [this issue] note that the SHZ appears to be along the western boundary of a regional conductivity anomaly. A further suggestion of possible structural control on the position of the SHZ is the observation that the hypocenters north of Mount St. Helens strike along the western boundary of the Spirit Lake pluton (compare Figures 1 and 5).

The May 1980 eruption indicates that magma volume in the brittle portion of the crust at Mount St. Helens is not constant. After the May 18, 1980, eruption, contraction of geodetic lines around Mount St. Helens was modeled as the result of a decrease in magma volume within the magma system below 7.0 km [*Scandone and Malone*, 1985], and this result suggested that magma withdrawn from the deeper reservoir was not completely replaced by magma from a still deeper reservoir. This interpretation is supported by our observation that earthquakes deeper than about 12 km along the northeast striking fault zone on May 18 tend to have nearly all dilational arrivals; qualitatively, this suggests that these events may have been the result of the collapse of magma-field volumes along the fault from which upward magma transport was not compensated with influx of new magma from a deeper source.

The volcanic history of Mount St. Helens indicates that as recently as the Kalama eruptive period (350–470 years before present), as much as 1–2 $km^3$ of magma was erupted [*Mullineaux and Crandell*, 1981; *Swanson et al.*, 1985]. This volume represents between 5 and 20% of the volume of 10–20 $km^3$ of magma estimated to be in the upper 20 km of the crust [*Scandone and Malone*, 1985]. If the influx of magma below 20 km is episodic and (as suggested by the seismicity and geodetic data) does not instantaneously replace magma withdrawn from the upper portion of the system, then the volume of magma stored in the upper 20 km of the crust may be subject to significant fluctuation even larger than those inferred to have occurred in 1980. Because the magma system is fault-bounded, one way for the volcanic system to compensate for short-term variations in magma volume is for slip to occur on the bounding faults.

The earthquake distribution beneath Mount St. Helens after the May 18 eruption indicates that at least some of this readjustment is seismic. However, the geodetic data indicate that readjustment of the volcanic ediface continued throughout the summer of 1980, with much of the change in slope distances occurring in June and July [*Swanson et al.*, 1981] when few earthquakes occurred (Figure 2). Although the deformation pattern was largely consistent with edifice contraction, *Swanson et al.* [1981] noted that two stations showed movement that was significantly different than simple contraction. They suggested that the motion of the stations Nelson and South Ridge (Figure 6), was consistent with right-lateral motion on a northwest striking fault.

To examine the hypothesis that right-lateral motion occurred on a northwest striking fault in terms of our model, we have plotted the base stations and the reflectors used by *Swanson et al.* [1981] on our model (Figure 6). Since with respect to the reflector South Ridge, it is clear that the target is on the opposite side of the fault zone striking to the southeast toward Marble Mountain (Figure 6), we conclude that the motion of this target is consistent with right-lateral slip on the proposed fault. As there are few earthquakes on this fault following the May 18 eruption, it appears that this slip after May 18 was largely aseismic. This slip which apparently occurred near the magma reservoir during June and July 1980 could have propagated along the fault and triggered the earthquakes at Marble Mountain.

To the east of the crater, the reflector at Nelson is near the projected position of the fault that bounds the eastern side of the magma reservoir, whereas the two base stations used to compute the motion are near the position of one of the north-south striking faults farther to the east (Figure 6). Thus shearing between these two faults would produce a counterclockwise rotation of the simple subsidence vector expected if volume adjustment was confined to a magma reservoir at depth.

Although our model is consistent with the observed geodetic data, the details of the readjustment around the magma volume is far from clear. As most of the geodetic data is consistent with volume collapse beneath the ediface, left-lateral motion (i.e., volume decrease) would be expected, if the fault adjustment were a simple process. The fact that right-lateral motion is observed indicates that more detailed modeling of the seismic data and geodetic measurements is needed to resolve the actual source of the fault motions. Despite the uncertainty as to the details of the source of the geodetic observations, we find the fit between the prediction of the seismicity model and the geodetic measurements as evidence that the adjustment of the magmatic system following the May 18, 1980, eruption involved both seismic and aseismic slip on the faults forming a dextral offset at Mount St. Helens. We note that geodetic data crossing the regional fault system at Mount St. Helens could be useful in detecting a future deep intrusion into the magma system that may not necessarily have concurrent seismicity.

## CONCLUSIONS

Mount St. Helens is located at a right-stepping offset in the St. Helens seismic zone (SHZ) and earthquake swarms related to volcanic eruptions occur within this offset. Because the SHZ is a right-lateral strike-slip fault, this offset creates a small volume under extension within the crust between the active fault segments. The offset of the SHZ at Mount St. Helens is similar to that observed for geothermal areas along the San Andreas fault system, where local crustal spreading occurs in areas oblique to the strike-slip faults. A model of the relation between the strike-slip zones and the crustal spreading centers observed along the San Andreas is applicable to Mount St. Helens once geometrical differences, expressed by the ratio of the fault offset ($l$) to the seismogenic depth ($h$), are taken into account. The spatial position of Mount St. Helens is likely controlled by the junction of the right-stepping offset of the SHZ with a set of fractures that predate the Quaternary volcanism. The older fractures are favorably aligned with respect to the contemporary stress directions for the transport of magma through the brittle portion of the crust.

*Acknowledgments.* This paper benefited from reviews by Dave Hill and Carl Johnson, an anonymous reviewer, and an Associate Editor. This work was funded by the U.S. Geological Survey's Geothermal, Volcano Hazards, and Earthquake Hazards programs.

## REFERENCES


Bacon, C. R., Implication of silicic vent patterns for the presence of large crustal magma chambers, *J. Geophys. Res.*, *90*, 11,243–11,252, 1985.

Bacon, C. R., W. A. Duffield, and K. Nakamura, Distribution of Quaternary rhyolite domes of the Coso Range, California: Implications for extent of the geomthermal anomaly, *J. Geophys. Res.*, *85*, 2425–2433, 1980.

Crosson, R. S., Small earthquakes, structure, and tectonics of the Puget Sound region, *Bull. Seismol. Soc. Am*, *62*, 1133–1171, 1972.

Duffield, W. A., C. R. Bacon, and B. G. Dalrymple, Late Cenozoic volcanism, geochronology, and structure of the Coso Range, Inyo County, California, *J. Geophys. Res.*, *85*, 2381–2404, 1980.

Endo, E. T., S. D. Malone, L. L. Noson, and C. S. Weaver, Locations, magnitudes, and statistics of the March 20–May 18 earthquake sequence, *U.S. Geol. Surv. Prof. Pap.*, *1250*, 93–107, 1981.

Evarts, R. C., R. P. Ashley, and J. G. Smith, Geology of Mount St. Helens area: Record of discontinuous volcanic and plutonic activity in the Cascade arc of southern Washington, *J. Geophys. Res.*, this issue.

Finn, C., and D. L. Williams, An areomagnetic study of Mount St. Helens, *J. Geophys. Res.*, this issue.

Fremont, M., and S. D. Malone, High precision relative locations of earthquakes at Mount St. Helens, Washington, *J. Geophys. Res.*, this issue.

Grant, W. C., and C. S. Weaver, Earthquakes near Swift Reservoir, Washington, 1958–1963: Seismicity along the southern St. Helens seismic zone, *Bull. Seismol. Soc. Am.*, *76*, 1573–1587, 1986.

Grant, W. C., C. S. Weaver, and J. E. Zollweg, The 14 February Elk Lake, Washington, earthquake sequence, *Bull. Seismol. Soc. Am.*, *74*, 1289–1309, 1984.

Hill, D. P., A model for earthquake swarms, *J. Geophys. Res.*, *82*, 1347–1352, 1977.

Jarrard, R. D., Relations among subduction parameters, *Rev. Geophys.*, *24*, 217–284, 1986.

Luedke, R. G., and R. L. Smith, Map showing distribution, composition, and age of late Cenozoic volcanic centers in Orgeon and Washington, *U.S. Geol. Surv. Map, I-1091-D*, 1982.

Malone, S. D., E. T. Endo, C. S. Weaver, and J. W. Ramey, Seismic monitoring for eruption prediction, *U.S. Geol. Surv. Prof. Pap.*, *1250*, 808–813, 1981.

Malone, S. D., C. Boyko, and C. S. Weaver, Seismic precursors to the Mount St. Helens eruptions in 1981 and 1982, *Science*, *221*, 1376–1378, 1983.

McNutt, S. R., and R. J. Beavan, Patterns of earthquakes and the effect of solid earth and ocean load tides at Mount St. Helens prior to the May 18, 1980, eruption, *J. Geophys. Res.*, *89*, 3075–3086, 1984.

Mullineaux, D. R., and D. R. Crandell, The eruptive history of Mount St. Helens, *U.S. Geol. Surv. Prof. Pap.*, *1250*, 3–15, 1981.

Nakamura, K., Volcanoes as possible indicators of tectonic stress orientation, *J. Volcanol. Geotherm. Res.*, *2*, 1–16, 1977.

Ode, H., Mechanical analysis of the dike pattern of the Spanish Peaks area, Colorado, *Geol. Soc. Am. Bull.*, *68*, 567–575, 1957.

Pollard, D. D., and O. H. Muller, The effect of gradients in regional stress and magma pressure on the form of sheet intrusions in cross section, *J. Geophys. Res.*, *81*, 975–984, 1976.

Scandone, R., and S. D. Malone, Magma supply, magma discharge, and readjustment of the feeding system of Mount St. Helens during 1980, *J. Volcanol. Geotherm. Res.*, *22*, 239–262, 1985.

Shemeta, J. E., and C. S. Weaver, Seismicity accompanying the May 18, 1980 eruption of Mount St. Helens, Washington, in *Mount St. Helens: Five Years Later*, edited by S. A. C. Keller, pp. 44–58, Eastern Washington University Press, Chency, 1986.

Stanley, W. D., C. Finn, and J. L. Plesha, Tectonics and conductivity structures in the southern Washington Cascades, *J. Geophys. Res.*, this issue.

Swanson, D. A., P. W. Lipman, J. G. Moore, C. C. Heliker, and K. M. Yamashita, Geodetic monitoring after the May 18 eruption, *U.S. Geol. Surv. Prof. Pap.*, *1250*, 347–377, 1981.

Swanson, D. A., T. J. Casadevall, D. Dzurisin, R. T. Holcomb, C. G. Newhall, S. D. Malone, and C. S. Weaver, Forecasts and predictions of eruptive activity at Mount St. Helens, USA: 1975–1984, *J. Geodyn. 3*, 397–423, 1985.

Weaver, C. S., and D. P. Hill, Earthquake swarms and local crustal spreading along major strike-slip faults in California, *Pure Appl. Geophys.*, *117*, 51–64, 1978/79.

Weaver, C. S., and S. W. Smith, Regional tectonic and earthquake hazard implications of a crustal fault zone in southwestern Washington, *J. Geophys. Res.*, *88*, 10,371–10,383, 1983.

Weaver, C. S., J. E. Zolleg, and S. D. Malone, Deep earthquakes beneath Mount St. Helens: Evidence for magmatic gas transport?, *Science*, *221*, 1391–1394, 1983.


W. C. Grant, J. E. Shemeta, and C. S. Weaver, U.S. Geological Survey, Geophysics Program AK-50, University of Washington, Seattle, WA 98195.

(Received April 17, 1986;
revised February 12, 1987;
accepted January 13, 1987.)